Intense hot Raman transitions within Renner–Teller states

Yehuda B. Band and B. Scharf

Citation: The Journal of Chemical Physics **79**, 3182 (1983); doi: 10.1063/1.446226
View online: http://dx.doi.org/10.1063/1.446226
View Table of Contents: http://scitation.aip.org/content/aip/journal/jcp/79/7?ver=pdfcov
Published by the AIP Publishing

Intense hot Raman transitions within Renner–Teller states

Yehuda B. Band and Benjamin Scharf

Department of Chemistry, Ben-Gurion University of the Negev, Beer-Sheva, Israel
(Received 2 July 1982; accepted 11 March 1983)

We analyze the hot Raman transitions within the split components of the first excited vibrational level of a Renner–Teller active mode in linear molecules. These transitions are predicted to be almost as intense as Rayleigh transitions and we expect them to be among the most prominent features of the Raman spectra. We describe the spectroscopic pattern, excitation profile, and depolarization ratio of Raman transitions within $^2\Pi$ Renner–Teller active states via $^2\Sigma$, $^2\Pi$, and $^2\Delta$ intermediate electronic states. We discuss these Raman transitions for the Renner–Teller case in the absence and presence of spin-orbit coupling.

I. INTRODUCTION

In this article we show that in Renner–Teller active states of linear molecules there exist Raman transitions within the split components of vibrationally excited levels of the active bending modes which are almost as intense as Rayleigh transitions, and therefore generally two to three orders of magnitude stronger than fundamental Raman transitions.[1] We expect these transitions to be among the most prominent features of the Raman spectra of Renner–Teller active states albeit the unfavorable Boltzmann factor.

We shall present the predicted intensity patterns, excitation profiles, and depolarization ratios of these hot Raman transitions in Renner–Teller active states of linear molecules with and without the presence of spin orbit interactions. The Raman transitions we consider are within the first excited vibrational level of the doubly degenerate bending modes in a doubly degenerate electronic state which is Renner–Teller active. The first excited vibrational level contains components that are split by the Renner–Teller interaction.[2,3] The transitions under consideration result from virtual excitation from the split components of these states to the excited electronic state manifold and emission back down to the various split components of the excited vibrational states. The reason that the strength of these transitions is generally much greater than fundamental Raman transitions is that these transitions have borrowed Rayleigh intensity. The frequency shifts of these Raman transitions result due to the splittings arising via the Renner–Teller interactions. Inclusion of spin-orbit interactions will further affect the nature of these Raman transitions.

The hot Raman transitions within this system are isomorphic to the hot Raman transitions recently predicted by us for quadratically Jahn–Teller active modes that are linearly inactive for molecules with D_{6h} symmetry.[4] Here we consider the case of a ground degenerate electronic state of a linear molecule with $^2\Pi$ symmetry. The bending vibrations of the linear molecule are doubly degenerate and these transverse vibrations have angular momentum with a nonzero component along the axis of the molecule. The vibronic interaction between the doubly degenerate electronic state and the doubly degenerate vibrational bending mode is known as the Renner–Teller interaction. This interaction removes some of the zeroth order degeneracies of the excited vibrational levels. In Sec. II we present a brief review of Renner–Teller interactions with and without the presence of spin-orbit coupling. In Sec. III we determine the nature of the Raman processes from the $^2\Pi$ Renner–Teller states via intermediate electronic states of $^2\Sigma$, $^2\Pi$, and $^2\Delta$ symmetry. In particular we shall be interested in Raman transitions within the first excited vibrational states of the degenerate bending modes and we shall investigate them in detail in the presence and in the absence of spin-orbit interactions because the intensities of these Raman transitions are extremely large despite the fact that they are hot transitions. We note that within the vibrationless level of a degenerate electronic ground state perturbed by spin-orbit coupling, intense Raman transitions within the split vibrationless level will also occur. These transitions yield information only regarding the spin-orbit interactions and do not reflect the nature of the Renner–Teller interactions which are exhibited in the hot transitions we discuss.

II. REVIEW OF RENNER-TELLER INTERACTIONS

We briefly review the analysis of Renner–Teller interactions.[2,3] This analysis will be presented for systems with and without the presence of spin-orbit coupling.

A. Renner-Teller without spin-orbit coupling

We consider a linear molecule with a doubly degenerate Π electronic ground state and containing a doubly degenerate vibrational bending mode. The two components of the electronic state can be denoted as Π^+ and Π^-, with projection of electronic angular momentum along the axis of the molecule Λ equal to ± 1. The two components of the doubly degenerate bending mode can be denoted as Q_+ and Q_-, with projection of nuclear vibrational angular momentum along the axis l equal to ± 1. In order to establish the isomorphism between this system and that of the quadratic Jahn–Teller interactions, in D_{6h} as presented in Ref. 4 we form the linear combinations

$$\Pi_x = \frac{1}{\sqrt{2}}(\Pi^+ + \Pi^-) , \tag{II.1}$$

$$\Pi_y = \frac{-i}{\sqrt{2}}(\Pi^+ - \Pi^-) , \tag{II.2}$$

 0021-9606/83/193182-08$02.10

$$Q_x = \frac{1}{\sqrt{2}}(Q_+ + Q_-) , \tag{II.3}$$

$$Q_y = \frac{-i}{\sqrt{2}}(Q_+ - Q_-) , \tag{II.4}$$

which are real representations of the electronic states and vibrational coordinates transforming under rotations about the linear axis as x and y, respectively.

The electronic Hamiltonian for this system is given by

$$H_e(q,Q) = H_e(q,Q_0) + \Delta V(q,Q) , \tag{II.5}$$

$$\Delta V(q,Q) = \left(\frac{\partial H_e}{\partial Q_x}\right)_{Q_0} Q_x + \left(\frac{\partial H_e}{\partial Q_y}\right)_{Q_0} Q_y + \frac{1}{2}\left[\left(\frac{\partial^2 H_e}{\partial Q_x^2}\right)_{Q_0} Q_x^2 + \left(\frac{\partial^2 H_e}{\partial Q_y^2}\right)_{Q_0} Q_y^2 + 2\left(\frac{\partial H_e}{\partial Q_x \partial Q_y}\right)_{Q_0} Q_x Q_y\right] , \tag{II.6}$$

where q denotes the electronic coordinates, Q denotes the nuclear coordinates, Q_0 is the linear nuclear equilibrium configuration, and where terms higher than quadratic in the bending mode are neglected. Symmetry considerations reveal that electronic matrix elements of ΔV are given by

$$\langle \Pi_x | \Delta V | \Pi_x \rangle = \tfrac{1}{2}(c+d)(Q_x^2 + Q_y^2) + \tfrac{1}{2}(c-d)(Q_x^2 - Q_y^2) , \tag{II.7}$$

$$\langle \Pi_y | \Delta V | \Pi_y \rangle = \tfrac{1}{2}(c+d)(Q_x^2 + Q_y^2) - \tfrac{1}{2}(c-d)(Q_x^2 - Q_y^2) , \tag{II.8}$$

$$\langle \Pi_x | \Delta V | \Pi_y \rangle = (c-d) Q_x Q_y , \tag{II.9}$$

where

$$c = \langle \Pi_x | \left(\frac{\partial^2 H_e}{\partial Q_x^2}\right)_{Q_0} | \Pi_x \rangle , \tag{II.10}$$

$$d = \langle \Pi_x | \left(\frac{\partial^2 H_e}{\partial Q_y^2}\right)_{Q_0} | \Pi_x \rangle . \tag{II.11}$$

We now diagonalize the vibronic Hamiltonian using basis functions of the form $\Pi_x[n_x, n_y]$ and $\Pi_y[n_x, n_y]$ where $[n_x, n_y]$ indicates the product of the zeroth order harmonic oscillator wave functions that are solutions to the zeroth order vibrational Hamiltonian which does not include the isotropic and anisotropic Renner–Teller interactions of Eqs. (II.7) and (II.8),

$$[n_x, n_y] = \psi_{n_x}(Q_x)\psi_{n_y}(Q_y) . \tag{II.12}$$

Alternatively, the isotropic terms in Eq. (II.7) and (II.8) could be included into the zeroth order vibrational wave function. Considering the $v = n_x + n_y = 1$ manifold specifically, the basis functions of the subset ($\Pi_x[10]$, $\Pi_y[01]$) interact with one another through the $Q_x Q_y$ terms of Eq. (II.9), and the basis functions of the subset ($\Pi_x[01]$, $\Pi_y[10]$) interact with one another through the same term, but there is no interaction between these two subsets. The diagonal matrix elements of the basis functions of the first subset are identical and equal to $[2(c+d) + (c-d)]\langle 0|Q^2|0\rangle$. The diagonal elements of the second subset are also identical and equal to $[2(c+d) - (c-d)]\langle 0|Q^2|0\rangle$. The off-diagonal interaction matrix elements in the two subsets equal $(c-d)\langle 0|Q|1\rangle\langle 1|Q|0\rangle = (c-d)\langle 0|Q^2|0\rangle$, which is half the separation energy between diagonal elements of the two subsets. Thus, the four $v = 1$ states which are degenerate in zeroth order split into three equally spaced levels. The middle level is doubly degenerate, whereas the upper and lower ones are nondegenerate. The splitting between the states equals $2(c-d)\langle 0|Q^2|0\rangle$. The resulting energy eigenfunctions and eigenvalues are given by

$$|\mathrm{I}\rangle = \frac{1}{\sqrt{2}}\{\Pi_x[10] + \Pi_y[01]\} , \quad E_{\mathrm{I}} = \bar{\omega} + 2[(c+d) + (c-d)]\langle 0|Q^2|0\rangle , \tag{II.13}$$

$$|\mathrm{II}\rangle = \frac{1}{\sqrt{2}}\{\Pi_x[10] - \Pi_y[01]\} , \quad E_{\mathrm{II}} = \bar{\omega} + 2(c+d)\langle 0|Q^2|0\rangle , \tag{II.14}$$

$$|\mathrm{III}\rangle = \frac{1}{\sqrt{2}}\{\Pi_x[01] + \Pi_y[10]\} , \quad E_{\mathrm{III}} = \bar{\omega} + 2(c+d)\langle 0|Q^2|0\rangle , \tag{II.15}$$

$$|\mathrm{IV}\rangle = \frac{1}{\sqrt{2}}\{\Pi_x[01] - \Pi_y[10]\} , \quad E_{\mathrm{IV}} = \bar{\omega} + 2[(c+d) - (c-d)]\langle 0|Q^2|0\rangle , \tag{II.16}$$

where $\bar{\omega}$ is the zero order frequency of the bending vibration. I is the lowest $v = 1$ state if $(c-d) < 0$, whereas IV is the lowest state if $(c-d) > 0$, and II and III comprise the middle doubly degenerate component. Here we have considered interactions between states of the $v = 1$ manifold. Inclusion of interactions between states of different v will not change the general pattern. In particular states II and III will remain degenerate as can be seen from symmetry considerations ($^2\Pi \otimes \pi = {}^2\Sigma^+ + {}^2\Sigma^- + {}^2\Delta$).

This analysis is isomorphic to that presented in Ref. 4 for quadratic Jahn–Teller interactions for molecules with D_{6h} symmetry.

B. Renner-Teller with spin-orbit coupling

We consider doublet spin states of the Renner–Teller vibronic levels presented above. The nonvanishing matrix elements of the spin-orbit coupling involve the operator $AL_z S_z$. For the $v = 1$ manifold there are eight vibronic-spin functions. Using the basis functions $|\mathrm{I}\rangle|\alpha\rangle$, $|\mathrm{II}\rangle|\alpha\rangle$, $|\mathrm{III}\rangle|\alpha\rangle$, $|\mathrm{IV}\rangle|\alpha\rangle$, and those with $|\alpha\rangle$ replaced by $|\beta\rangle$ the Hamiltonian including spin-orbit can be diagonalized within the $v = 1$ manifold. The basis functions containing $|\alpha\rangle$ do not interact with those containing $|\beta\rangle$. Moreover, the basis states involving (I, IV) do not interact with (II, III). Diagonalizing, one obtains the eigenfunctions

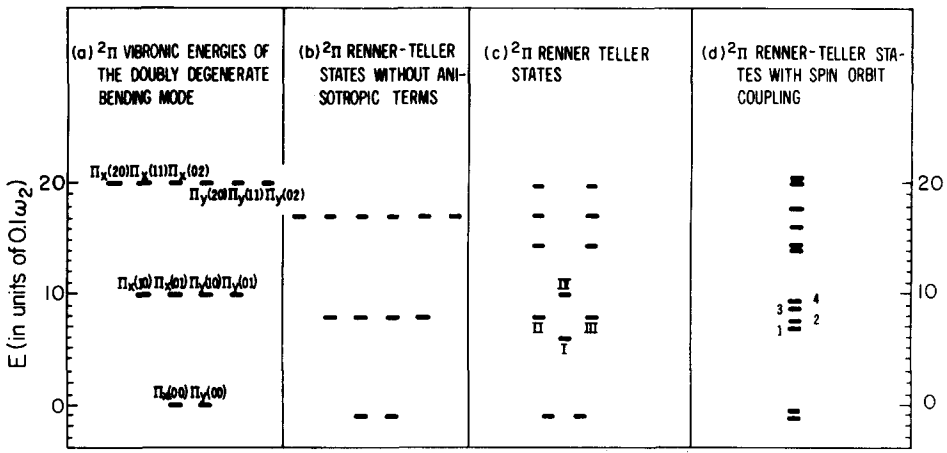

FIG. 1. Energy levels of Renner–Teller active vibronic states of $^2\Pi$ electronic state. Π_x, Π_y denote the two degenerated electronic components and $[n_a, n_b]$ denote the quantum numbers in the two degenerate components of the bending modes Q_a, Q_b. The parameters c and d of Eqs. (II.10) and (II.11) are taken as $c = -\omega/(10\langle 0|Q^2|0\rangle)$ and $d = 0$. The spin-orbit coupling constant A is taken as $A = 2|c|\langle 0|Q^2|0\rangle$.

$$
\begin{aligned}
|1\rangle &= |\cos\theta\,\mathrm{I} + i\sin\theta\,\mathrm{IV}\rangle|\alpha\rangle\ , \\
|2\rangle &= \frac{1}{\sqrt{2}}\,|\mathrm{II} - i\,\mathrm{III}\rangle|\alpha\rangle\ , \\
|3\rangle &= \frac{1}{\sqrt{2}}\,|\mathrm{II} + i\,\mathrm{III}\rangle|\alpha\rangle\ , \\
|4\rangle &= |i\sin\theta\,\mathrm{I} + \cos\theta\,\mathrm{IV}\rangle|\alpha\rangle\ , \qquad \text{(II.17)} \\
|\bar{1}\rangle &= |\cos\theta\,\mathrm{I} - i\sin\theta\,\mathrm{IV}\rangle|\beta\rangle\ , \\
|\bar{2}\rangle &= \frac{1}{\sqrt{2}}\,|\mathrm{II} + i\,\mathrm{III}\rangle|\beta\rangle\ , \\
|\bar{3}\rangle &= \frac{1}{\sqrt{2}}\,|\mathrm{II} - i\,\mathrm{III}\rangle|\beta\rangle\ , \\
|\bar{4}\rangle &= |-i\sin\theta\,\mathrm{I} + \cos\theta\,\mathrm{IV}\rangle|\beta\rangle\ , \qquad \text{(II.18)}
\end{aligned}
$$

where the angle θ is given by the relation

$$\theta = \tan^{-1}\left(\frac{E_{\mathrm{IV}} - E_{\mathrm{I}} - \sqrt{(E_{\mathrm{IV}} - E_{\mathrm{I}})^2 + A^2}}{A}\right)\ ,$$

and corresponding eigenvalues

$$
\begin{aligned}
E_1 &= E_{\bar{1}} = \tfrac{1}{2}(E_{\mathrm{I}} + E_{\mathrm{IV}} - \sqrt{(E_{\mathrm{IV}} - E_{\mathrm{I}})^2 + A^2})\ , \\
E_2 &= E_{\bar{2}} = E_{\mathrm{II}} - \tfrac{1}{2}A\ , \\
E_3 &= E_{\bar{3}} = E_{\mathrm{II}} + \tfrac{1}{2}A\ , \\
E_4 &= E_{\bar{4}} = \tfrac{1}{2}(E_{\mathrm{I}} + E_{\mathrm{IV}} + \sqrt{(E_{\mathrm{IV}} - E_{\mathrm{I}})^2 + A^2})\ . \qquad \text{(II.19)}
\end{aligned}
$$

Figure 1 shows the energy eigenvalue pattern for $v = 0$, 1, 2 with and without spin-orbit coupling.

III. HOT RAMAN TRANSITIONS WITHIN $v = 1$ MANIFOLD

A. Without spin-orbit coupling

We consider the Raman scattering in the off-resonance regime for various intermediate electronic scattering states. The Raman polarizability tensor $\alpha_{FG}(\omega_0)_{\rho\sigma}$ between initial and final states $|G\rangle$ and $|F\rangle$ for incident photon energy ω_0 is given by

$$\alpha_{FG}(\omega_0)_{\rho\sigma} = \sum_J \frac{\langle F|R_\rho|J\rangle\langle J|R_\sigma|G\rangle}{E_J - E_G - \omega_0} + \frac{\langle F|R_\sigma|J\rangle\langle J|R_\rho|G\rangle}{E_J - E_F + \omega_0}\ . \qquad \text{(III.1)}$$

Here R_σ is the σ component of the dipole moment operator, E_M denotes the energy of vibronic state $|M\rangle$, and $|J\rangle$ are a complete set of vibronic states excluding the initial and final states. Neglecting the vibrational energy contributions to the energy denominators in Eq. (III.1) (which is valid in the off-resonance and pre-resonance regime) *and* using closure to express the sum over all intermediate vibrational states, Eq. (III.1) takes the form[5]

$$\alpha_{FG}(\omega_0)_{\rho\sigma} = \sum_{J_{\mathrm{el}}}\left\{\frac{1}{E_{J_{\mathrm{el}}} - E_{G_{\mathrm{el}}} - \omega_0}\langle\langle F|R_\rho|J_{\mathrm{el}}\rangle_q\langle J_{\mathrm{el}}|R_\sigma|G\rangle_q\rangle_Q + \frac{1}{E_{J_{\mathrm{el}}} - E_{E_{\mathrm{el}}} + \omega_0}\langle\langle F|R_\sigma|J_{\mathrm{el}}\rangle_q\langle J_{\mathrm{el}}|R_\rho|G\rangle_q\rangle_Q\right\}. \qquad \text{(III.2)}$$

Here $|J_{\mathrm{el}}\rangle$ is the electronic wave function of the intermediate state $|J\rangle$ and the brackets with a q subscript indicate integration over electronic coordinates whereas the brackets with a Q subscript indicate integration over nuclear coordinates. In the resonance Raman regime the approximation leading to Eq. (III.2) are not valid and other methods must be employed.

The total intensity for the Raman transitions from $|G\rangle$ to $|F\rangle$ with incident frequency ω_0 is given by[6,7]

$$I_{FG} = \frac{2^3\pi}{3^2c^4}\,\omega^4 I_0 \sum_{\rho\sigma}|\alpha_{FG}(\omega_0)_{\rho\sigma}|^2\ , \qquad \text{(III.3a)}$$

where I_0 is the incident field intensity with frequency ω_0, and ω is the scattered light frequency. Considering the case where the incident light is unpolarized and one measures the scattered light propagating in a plane perpendicular to that of the incident light, the depolarization ratio ρ_n is defined as the ratio of the intensity of the scattered light polarized perpendicular to the perpendicular plane to that polarized parallel to this plane. The depolarization ratio for a Raman transition from G to F is given in terms of the Raman polarizability tensor by the expression[6,7]

$$\rho_n = \frac{\sum_{\rho\sigma}[6|\alpha^S_{FG}(\omega_0)_{\rho\sigma}|^2 + 10|\alpha^A_{FG}(\omega_0)_{\rho\sigma}|^2]}{\sum_{\rho\sigma}[10|\alpha^0_{FG}(\omega_0)_{\rho\sigma}|^2 + 7|\alpha^S_{FG}(\omega_0)_{\rho\sigma}|^2 + 5|\alpha^A_{FG}(\omega_0)_{\rho\sigma}|^2]}\ , \qquad \text{(III.3b)}$$

where the isotropic, symmetric, and antisymmetric tensors are given by

$$\alpha^0_{\rho\sigma} = (\mathrm{Tr}\,\alpha/3)\,\delta_{\rho\sigma}\ , \tag{III.4}$$

$$\alpha^s_{\rho\sigma} = \tfrac{1}{2}(\alpha_{\rho\sigma} + \alpha_{\sigma\rho}) - (\mathrm{Tr}\,\alpha/3)\,\delta_{\rho\sigma}\ , \tag{III.5}$$

$$\alpha^A_{\rho\sigma} = \tfrac{1}{2}(\alpha_{\rho\sigma} - \alpha_{\sigma\rho})\ . \tag{III.6}$$

Let us now consider the Stokes and anti-Stokes Raman transitions within the $v = 1$ manifold II $\leftarrow$ I, III $\leftarrow$ I, IV $\leftarrow$ I, IV $\leftarrow$ II, IV $\leftarrow$ III, and I $\leftarrow$ II, I $\leftarrow$ III, II $\leftarrow$ IV, III $\leftarrow$ IV as well as the Raman transitions III $\leftarrow$ II, II $\leftarrow$ III for which $\omega = \omega_0$. The intensity and the depolarization ratios of these transitions as well as their dependence on incident photon frequency will be obtained. It will become apparent from the discussion below, that the polarizability tensors of these Raman transitions are of comparable strength to those of Rayleigh transitions and they are generally about 1000 times larger than those of fundamental Raman transitions. Despite the Boltzmann factors for the population of the $v = 1$ manifold which reduces the spectral intensity of these Raman transitions in comparison with Rayleigh scattering, these Raman transitions will be as intense as the fundamental Raman transitions even when the Boltzmann factor is ~ 1/1000. We consider excited electronic states for configurations near the equilibrium configuration of the ground state, expanding in a complete set of electronic states of linear molecules. Symmetry considerations reveal that the only electronic states which carry oscillator strength via the electric dipole moment operator from $^2\Pi$ electronic states are $^2\Sigma$, $^2\Pi$, and $^2\Delta$ electronic states. In addition to the isomorphism between Renner–Teller $^2\Pi$ states and quadratically Jahn–Teller active ^2E states in D_{6h} symmetry, there is an isomorphism between the transition dipole matrix elements in the two cases. More specifically, for dipole transitions from a $^2E_{2u}$ state in D_{6h} symmetry, the matrix elements to $^2B_{2g}$, $^2E_{2g}$, and $^2E_{1g}$ are isomorphic to the dipole transition matrix elements from a $^2\Pi$ state to $^2\Sigma$, $^2\Pi$, and $^2\Delta$ in linear molecules. Consequently, the pattern of the Raman spectra for these two cases will be identical. This similarity of the Raman transitions holds for the Raman intensities, depolarization ratios, and excitation profiles of the corresponding transitions. In the following we summarize the results for Raman transitions within the $v = 1$ manifold of Renner–Teller states for the various intermediate electronic states in the absence of spin-orbit-coupling. In Sec. III B we extend our investigation and explore the effects of spin-orbit interactions on these hot Raman transitions.

1. $^2\Pi$ ground electronic state and $^2\Sigma$ intermediate electronic state

Using Eq. (III. 2) and the equality of electronic dipole transition matrix elements, $\tau = \langle {}^2\Sigma\,|\,x\,|\,{}^2\Pi_x\rangle = \langle {}^2\Sigma\,|\,y\,|\,{}^2\Pi_y\rangle$ and noting that $\langle {}^2\Sigma\,|\,x\,|\,\Pi_y\rangle = \langle {}^2\Sigma\,|\,y\,|\,{}^2\Pi_x\rangle = 0$, we obtain the relations for the Raman intensities and depolarization ratios for Raman transitions within the $v = 1$ manifold:

$$I_{\mathrm{II}\leftarrow\mathrm{I}} = I_{\mathrm{III}\leftarrow\mathrm{I}} = I_{\mathrm{IV}\leftarrow\mathrm{II}} = I_{\mathrm{IV}\leftarrow\mathrm{III}} = I_{\mathrm{I}\leftarrow\mathrm{II}} = I_{\mathrm{I}\leftarrow\mathrm{III}} = I_{\mathrm{II}\leftarrow\mathrm{IV}} = I_{\mathrm{III}\leftarrow\mathrm{IV}} = \frac{2^3\pi}{3^2c^4}\,\omega^4 I_0\,\frac{2(\Delta E)^2\tau^4}{[(\Delta E)^2 - \omega_0^2]^2}\ . \tag{III.7}$$

The depolarization ratio ρ_n for all these transitions is equal to 6/7 (since the polarizability tensor for these transitions is symmetric and traceless). The intensity of the remaining transitions is given by

$$I_{\mathrm{III}\leftarrow\mathrm{II}} = I_{\mathrm{IV}\leftarrow\mathrm{I}} = I_{\mathrm{II}\leftarrow\mathrm{III}} = I_{\mathrm{I}\leftarrow\mathrm{IV}} = \frac{2^3\pi}{3^2c^4}\,\omega^4 I_0\,\frac{2\omega_0^2\tau^4}{[(\Delta E)^2 - \omega_0^2]^2}\ . \tag{III.8}$$

The depolarization ratio for the transitions in Eq. (III. 8) is equal to 2 (since the polarizability tensor for these transitions is antisymmetric). Figure 2(a) shows the Raman spectrum and depolarization ratios for this case. The transitions II $\leftarrow$ I, III $\leftarrow$ I, IV $\leftarrow$ II, and IV $\leftarrow$ III appear at $\omega = \omega_0 + 2(c-d)\,\langle 0\,|\,Q^2\,|\,0\rangle \equiv \omega_0 - \Delta\omega$, the transition IV $\leftarrow$ I appears at $\omega = \omega + 4(c-d)\,\langle 0\,|\,Q^2\,|\,0\rangle \equiv \omega - 2\Delta\omega$, the transition III $\leftarrow$ II appears on top of the Rayleigh frequency, and the reversed transitions and clearly shifted from ω_0 by the same shift but with opposite sign.

To obtain the spectral intensity of a transition $F \leftarrow G$ the intensity $I_{F\leftarrow G}$ should be multiplied by the Boltzmann factor for state G.

The Raman transitions which are reverse polarized ($\rho_n = 2$) I $\rightleftharpoons$ IV and II $\rightleftharpoons$ III will display a different excitation profile than the depolarized transitions ($\rho_n = 6/7$) I $\rightleftharpoons$ II, I $\rightleftharpoons$ III, II $\rightleftharpoons$ IV, and III $\rightleftharpoons$ IV as can be seen from Eqs. (III. 7) and (III. 8). The intensity of the reverse polarized transitions increases faster than those of the depolarized transitions as the frequency of the incident light increases. For $\Delta E > \omega_0$ the intensity of the depolarized transitions is stronger than the reverse polarized transitions, whereas the opposite prevails for $\Delta E < \omega_0$.

2. $^2\Pi$ ground electronic state and $^2\Sigma$ intermediate electronic state

A similar treatment to that of the previous section can be carried out using an intermediate electronic state of symmetry $^2\Pi$. We denote the two components of the intermediate $^2\Pi$ state which transform as x and y under rotations about the axis of the molecule by Φ_x and Φ_y. Dipole transitions from the ground $^2\Pi$ to the excited $^2\Pi$ state are polarized in the z direction. The component Π_x of the ground state is coupled through z to the Φ_x component of the excited state, and the Π_y component is coupled through z to Φ_y. The approximations leading to Eq. (III. 2), when applied here yield

$$\alpha_{FG}(\omega_0) = \frac{1}{E_{\Pi_{ex}} - E_{\Pi_g} - \omega_0}\,\langle\langle F\,|\,z\{\,|\,\Phi_x\rangle_Q\langle\Phi_x\,|\,+\,|\,\Phi_y\rangle_Q\langle\Phi_y\,|\}\,z\,|\,G\rangle_g\rangle_Q + \frac{1}{E_{\Pi_{ex}} - E_{\Pi_g} + \omega_0}\,\langle\langle F\,|\,z\{\,|\,\Phi_x\rangle_Q\langle\Phi_x\,|\,+\,|\,\Phi_y\rangle_Q\langle\Phi_y\,|\}\,z\,|\,G\rangle_Q\rangle_Q\ . \tag{III.9}$$

Using Eq. (III. 9) and the fact that $|\langle\Phi_x\,|\,z\,|\,\Pi_x\rangle| = |\langle\Phi_y\,|\,z\,|\,\Pi_y\rangle|$ it is easy to find that all the hot Raman transitions within the $v = 1$ manifold vanish. Thus, intermediate $^2\Pi$ states do not contribute to the intensity of these Raman transitions.

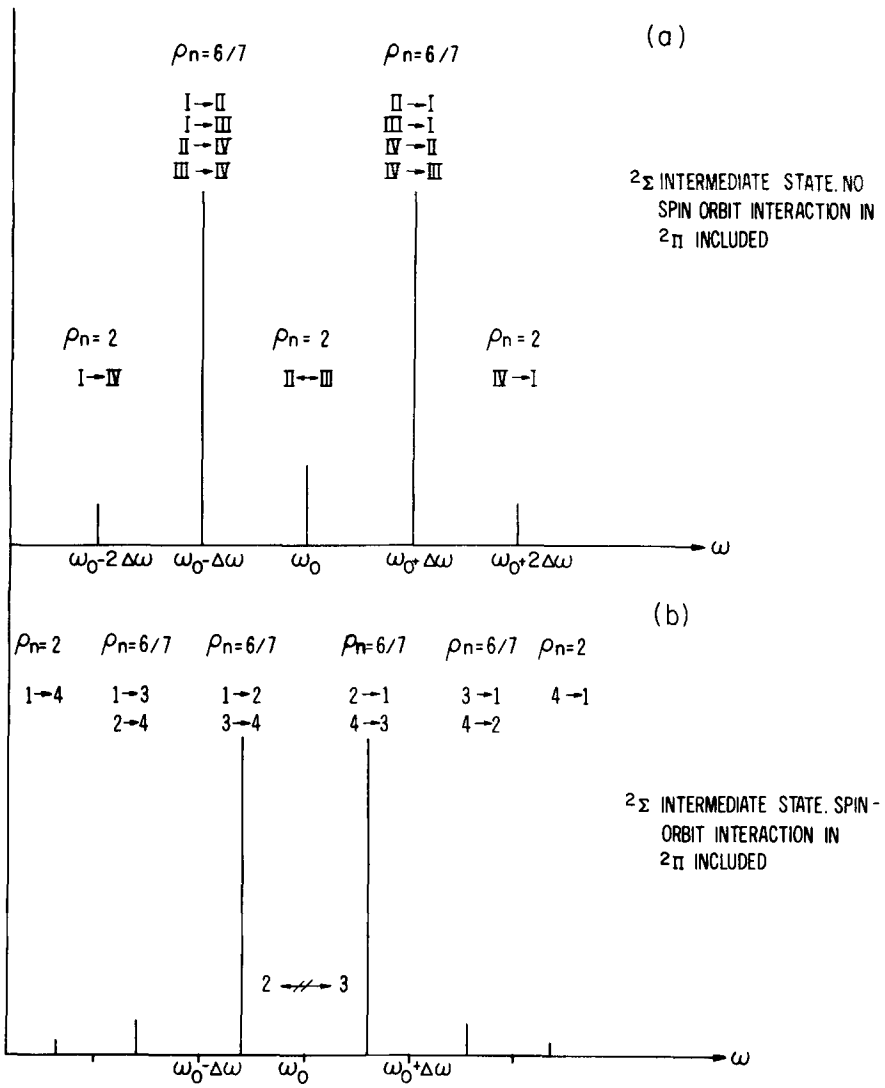

FIG. 2. Raman spectrum and depolarization ratios of the transitions within the $v=1$ manifold of a quadratically Renner-Teller active mode when the intermediate scattering state is of $^2\Sigma$ symmetry. The Boltzmann factors of the initial state are not incorporated into the intensities given here. We have arbitrarily used $\omega_0 = 2/3\ (E_{^2\Sigma} - E_{^2\Pi})$. The results are given for the Renner–Teller case with and without spin-orbit coupling.

3. $^2\Pi$ *ground electronic state and* $^2\Delta$ *intermediate electronic state*

We define two components of the $^2\Delta$ state by $\Delta_1 = (\Delta_{+2} + \Delta_{-2})/2$ and $\Delta_2 = (\Delta_{+2} - \Delta_{-2})/2i$. The Π_x component of the $^2\Pi$ ground state couples with Δ_1 through x, whereas the Π_x component couples with Δ_2 through y. The Π_y component couples with Δ_1 through y and with Δ_2 through x.

The following relations hold for these matrix elements:

$$\langle\Delta_1|x|\Pi_x\rangle = \langle\Delta_2|y|\Pi_x\rangle = \langle\Delta_2|x|\Pi_y\rangle = -\langle\Delta_1|y|\Pi_y\rangle \ . \quad \text{(III. 10)}$$

The approximations leading to Eq. (III. 2), when applied here yield

$$\alpha_{FG}(\omega_0)_{\rho\sigma} = \frac{1}{E_\Delta - E_\Pi - \omega_0}\langle\langle F|R_\rho\{|\Delta_1\rangle_q\langle\Delta_1| + |\Delta_2\rangle_q\langle\Delta_2|\}R_\sigma|G\rangle_q\rangle_Q + \frac{1}{E_\Delta - E_\Pi + \omega_0}\langle\langle F|R_\sigma\{|\Delta_1\rangle_q\langle\Delta_1| + |\Delta_2\rangle_q\langle\Delta_2|\}R_\rho|G\rangle_q\rangle_Q \ . \quad \text{(III. 11)}$$

Using this expression it is easy to show that

$$I_{IV\to I} = I_{I\to IV} = I_{III\to II} = I_{II\to III} = \frac{2^3\pi}{3^2c^4}\,\omega^4 I_0\,\frac{2\omega_0^2\tilde{\tau}^4}{[(\Delta E)^2 - \omega_0^2]^2} \ , \quad \text{(III. 12)}$$

where

$$\tilde{\tau} = |\langle\Delta_1|x|\Pi_x\rangle| \quad \text{(III. 13)}$$

and

$$\widetilde{\Delta E} = E_\Delta - E_\Pi \ . \quad \text{(III. 14)}$$

Furthermore, the depolarization ratio ρ_n for all these transitions is equal to 2. In contradistinction with the case of a $^2\Sigma$ intermediate state, here there are no Raman transitions between I⇔II, I⇔III, II⇔IV, and III⇔IV. Thus, the only transitions appearing in the Raman spectrum are the Stokes and anti-Stokes at $\omega = \omega_0 \pm 2\Delta\omega$. These transitions are reverse polarized [see Fig. 3(a)].

B. Renner-Teller with spin-orbit coupling

We now consider the Raman intensity and depolarization ratios for the hot Raman transitions within the $v=1$ manifold of the $^2\Pi$ electronic ground state split by the

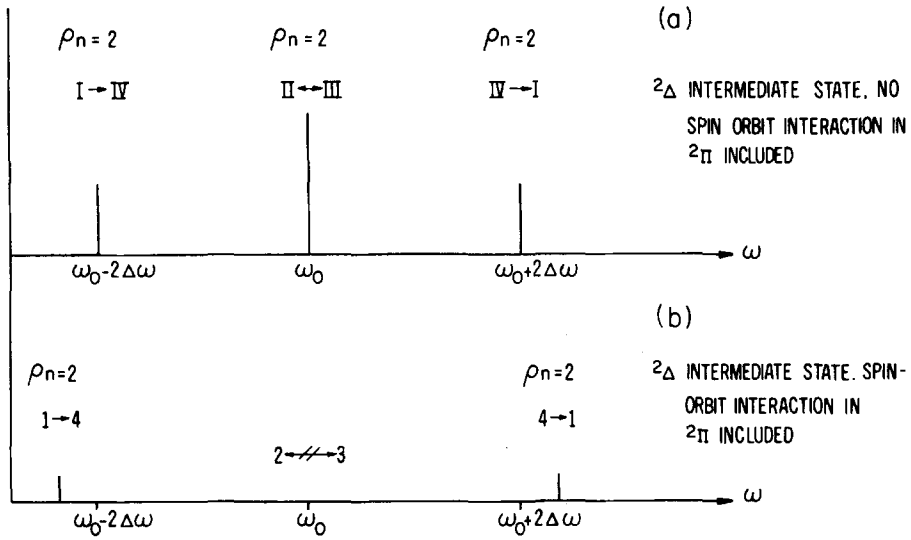

FIG. 3. Raman spectrum and depolarization ratios of the transitions within the $v = 1$ manifold of a quadratically Renner–Teller active mode when the intermediate scattering state is of $^2\Delta$ symmetry. The Boltzmann factors of the initial state are not incorporated into the intensities given here. The results are given for the Renner–Teller case with and without spin-orbit coupling.

spin-orbit interaction using the states constructed in Sec. II B and the results without spin-orbit coupling of the previous subsection.

The vibronic functions of the initial and final states $|G\rangle$, $|F\rangle = |1\rangle$, $|2\rangle$, $|3\rangle$, $|4\rangle$, $|\bar{1}\rangle$, $|\bar{2}\rangle$, $|\bar{3}\rangle$, and $|\bar{4}\rangle$ are linear combinations of the basis states I, II, III, and IV as specified in Eqs. (II. 17) and (II. 18). Substituting the linear combinations for $|G\rangle$ and $|F\rangle$, and noting that an initial state with spin function $|\alpha\rangle(|\beta\rangle)$ combines only with intermediate and final states with spin function $|\alpha\rangle(|\beta\rangle)$, we obtain the components of the polarizability tensor $(\alpha_{ij})_{GF}$ as linear combinations of the components of the polarizability tensor for the basis states I, II, III, and IV. Thus,

$$(\alpha_{ij})_{2\leftarrow 1} = \left(\frac{\cos\theta - \sin\theta}{\sqrt{2}}\right)[(\alpha_{ij})_{\mathrm{II}\leftarrow \mathrm{I}} + i(\alpha_{ij})_{\mathrm{III}\leftarrow \mathrm{I}}] = (\alpha_{ij})^*_{\bar{1}\leftarrow 2} ,$$

$$(\alpha_{ij})_{3\leftarrow 1} = \left(\frac{\cos\theta + \sin\theta}{\sqrt{2}}\right)[(\alpha_{ij})_{\mathrm{II}\leftarrow \mathrm{I}} + i(\alpha_{ij})_{\mathrm{III}\leftarrow \mathrm{I}}] = (\alpha_{ij})^*_{\bar{1}\leftarrow 3} ,$$

$$(\alpha_{ij})_{4\leftarrow 1} = (\cos^2\theta - \sin^2\theta)\,(\alpha_{ij})_{\mathrm{IV}\leftarrow \mathrm{I}} = -(\alpha_{ij})_{\bar{1}\leftarrow 4} ,$$

$$(\alpha_{ij})_{3\leftarrow 2} = 0 = (\alpha_{ij})_{2\leftarrow 3} ,$$

$$(\alpha_{ij})_{\bar{2}\leftarrow \bar{1}} = (\alpha_{ij})^*_{\bar{1}\leftarrow \bar{2}} = (\alpha_{ij})^*_{2\leftarrow 1} ,$$

$$(\alpha_{ij})_{\bar{3}\leftarrow \bar{1}} = (\alpha_{ij})^*_{\bar{1}\leftarrow \bar{3}} = (\alpha_{ij})^*_{3\leftarrow 1} ,$$

$$(\alpha_{ij})_{\bar{4}\leftarrow \bar{1}} = -(\alpha_{ij})_{\bar{1}\leftarrow \bar{4}} = (\alpha_{ij})^*_{4\leftarrow 1} , \qquad \text{(III. 15)}$$

$$(\alpha_{ij})_{\bar{3}\leftarrow \bar{2}} = (\alpha_{ij})_{\bar{2}\leftarrow \bar{3}} = 0 ,$$

where we have used the relations

$$(\alpha_{ij})_{\mathrm{II}\leftarrow \mathrm{I}} = (\alpha_{ij})_{\mathrm{I}\leftarrow \mathrm{II}} = (\alpha_{ij})_{\mathrm{III}\leftarrow \mathrm{IV}} = (\alpha_{ij})_{\mathrm{IV}\leftarrow \mathrm{III}} ,$$

$$(\alpha_{ij})_{\mathrm{III}\leftarrow \mathrm{I}} = (\alpha_{ij})_{\mathrm{I}\leftarrow \mathrm{III}} = -(\alpha_{ij})_{\mathrm{II}\leftarrow \mathrm{IV}} = -(\alpha_{ij})_{\mathrm{IV}\leftarrow \mathrm{II}} ,$$

$$(\alpha_{ij})_{\mathrm{IV}\leftarrow \mathrm{I}} = -(\alpha_{ij})_{\mathrm{I}\leftarrow \mathrm{IV}} ,$$

$$(\alpha_{ij})_{\mathrm{III}\leftarrow \mathrm{II}} = -(\alpha_{ij})_{\mathrm{II}\leftarrow \mathrm{IV}} ,$$

$$(\alpha_{ij})_{\mathrm{I}\leftarrow \mathrm{I}} = (\alpha_{ij})_{\mathrm{II}\leftarrow \mathrm{II}} = (\alpha_{ij})_{\mathrm{III}\leftarrow \mathrm{III}} = (\alpha_{ij})_{\mathrm{IV}\leftarrow \mathrm{IV}} . \qquad \text{(III. 16)}$$

These relations hold for all the intermediate states $^2\Sigma$, and $^2\Pi$, and $^2\Delta$, which carry dipole allowed oscillator strength from the $^2\Pi$ ground state. Using relations (III. 15) and (III. 16), noting that $(\alpha_{ij})_{\mathrm{II}\leftarrow \mathrm{I}}$ and $(\alpha_{ij})_{\mathrm{III}\leftarrow \mathrm{I}}$ have no nonvanishing elements in common, and applying the results of Sec. III A for the polarizability tensors connecting the basis functions I, II, III, and IV for all intermediate states, we obtain the following results.

For a $^2\Sigma$ intermediate state, the Raman scattering pattern is shown in Fig. 2. The intensity of the Stokes transition $2 \leftarrow 1$ is given by

$$I_{2\leftarrow 1} = (\cos\theta - \sin\theta)^2 I_{\mathrm{III}\leftarrow \mathrm{I}}$$

$$= \frac{2^3\pi}{3^2 c^4}\,\omega^4 I_0\,(\cos\theta - \sin\theta)^2\,\frac{2(\Delta E)^2\tau^4}{[(\Delta E)^2 - \omega_0^2]^2} , \qquad \text{(III. 17)}$$

and the transition appears at frequency $\omega = \omega_0 - (E_2 - E_1) = \omega_0 - (\sqrt{(E_{\mathrm{IV}} - E_{\mathrm{I}})^2 + A^2} - A)/2$. The depolarization ratio for $2 \leftarrow 1$ is $\rho_n = 6/7$. The transition $4 \leftarrow 3$ appears at the same position as $2 \leftarrow 1$ with intensity equal to that of $2 \leftarrow 1$,

$$I_{4\leftarrow 3} = I_{2\leftarrow 1} \qquad \text{(III. 18)}$$

and with depolarization ratio $\rho_n = 6/7$.

The Stokes transitions $3 \leftarrow 1$ and $4 \leftarrow 2$ appear at $\omega = \omega_0 - (\sqrt{(E_{\mathrm{IV}} - E_{\mathrm{I}})^2 + A^2} + A)/2$ with intensities

$$I_{3\leftarrow 1} = I_{4\leftarrow 2} = (\cos\theta + \sin\theta)^2 I_{\mathrm{II}\leftarrow \mathrm{I}}$$

$$= \frac{2^3\pi}{3^2 c^4}\,\omega^4 I_0 (\cos\theta + \sin\theta)^2\,\frac{2(\Delta E)^2\tau^4}{[(\Delta E)^2 - \omega_0^2]^2} \qquad \text{(III. 19)}$$

and $\rho_n = 6/7$.

The Stokes transition $4 \leftarrow 1$ appears at $\omega = \omega_0 - \sqrt{(E_{\mathrm{IV}} - E_{\mathrm{I}})^2 + A^2}$. Its intensity is

$$I_{4\leftarrow 1} = (\cos^2\theta - \sin^2\theta)^2 I_{\mathrm{IV}\leftarrow \mathrm{I}}$$

$$= \frac{2^3\pi}{3^2 c^4}\,\omega^4 I_0 (\cos^2\theta - \sin^2\theta)^2\,\frac{2\omega_0^2\tau^4}{[(\Delta E)^2 - \omega_0^2]^2} . \qquad \text{(III. 20)}$$

and ρ_n for this transition equals 2 (reverse polarized).

The Stokes transition $3 \leftarrow 2$ has vanishing Raman intensity. The anti-Stokes transitions obtained by reversing the arrow on the corresponding Stokes transitions have identical intensities and depolarization ratios as the Stokes transitions. The transitions labeled with bars ($|\beta\rangle$ spin state manifold) are identical in every re-

spect to the unbarred transitions.

There are no contributions to Raman scattering within the $v = 1$ manifold via a $^2\Pi$ intermediate state. This occurs because the polarizability tensors connecting the states diagonalizing Renner-Teller and spin-orbit couplings are linear combinations of the polarizability tensors connecting the states I, II, III, IV, and these polarizability tensors vanish for $^2\Pi$ intermediate states.

The contribution to Raman scattering within $v = 1$ via a $^2\Delta$ intermediate state can be obtained using the results of Sec. III A 3. We find that the transitions $3 \rightleftharpoons 2$ vanish and the only nonvanishing Raman transitions are $1 \rightleftharpoons 4$ (see Fig. 3) which have intensities

$$I_{4\to1} = I_{1\to4} = \frac{2^3\pi}{3^2c^4}\,\omega^4 I_0(\cos^2\theta - \sin^2\theta)^2 \times \frac{2\omega_0^2\tilde{\tau}^4}{[(\widetilde{\Delta E})^2 - \omega_0^2]^2} \qquad \text{(III. 21)}$$

and depolarization ratios equal to 2. The whole intensity that was in the transitions III $\rightleftharpoons$ II returns to the Rayleigh transitions $2 \rightleftharpoons 2$, $3 \rightleftharpoons 3$. Thus the Rayleigh polarizability tensor contains antisymmetric contributions. In the limit as $|A| \gg |E_{IV} - E_I|$, $(\cos^2\theta - \sin^2\theta)$ tends to zero, so the intensities of the remaining Raman transitions $1 \rightleftharpoons 4$ become small in this limit. This is also true for the $1 \rightleftharpoons 4$ transitions via $^2\Sigma$ intermediates.

For the vibrationless state, the eigenstates split into two doubly degenerate components viz. ($|\Pi^-[00]\alpha\rangle$, $|\Pi^+[00]\beta\rangle$) and ($|\Pi^+[00]\alpha\rangle$, $|\Pi^-[00]\beta\rangle$) and the energy separation between them equals the spin-orbit coupling constant A. Recall that the splitting between states 2 and 3 also equals A. The Raman transitions between 2 and 3 have vanishing intensity whereas the Raman transitions between $|\Pi^-[00]\alpha\rangle$ and $|\Pi^+[00]\alpha\rangle$ occur and have high intensity due to their Rayleigh-like character. One thereby learns the strength of the spin orbit coupling constant from this Raman line.

IV. CONCLUSION

We demonstrated the presence of very intense hot Raman transitions within the manifold of the split $v = 1$ level of vibronically active bending modes in Renner-Teller active states of linear molecules. We discussed the intensity pattern, depolarization ratio, and excitation profile for these Raman transitions in the case of Renner-Teller interactions excluding spin-orbit coupling and including spin-orbit coupling for $^2\Pi$ electronic states. The pattern of the hot Raman transitions was elucidated for all intermediate states possible. An important feature of these transitions is their outstandingly strong intensity. They are expected to be a prominent feature in the Raman spectrum albeit the fact that their spectral intensity is attenuated by an unfavorable Boltzmann factor. We have analyzed the Raman spectrum for these transitions in the off-resonance and preresonance regime. The analysis for the resonance case can be developed on the basis of our present discussion and the analysis using Green's function methods for resonance Raman scattering[8] but we did not pause to do so. It is evident, however, that the Raman transitions within the split $v = 1$ manifold of Renner-Teller active bending modes in linear molecules will be an important feature in the resonance-Raman regime as well. For the molecules BO_2, N_3, CO_2^+, NCO, NCS, etc., one encounters Renner-Teller splittings up to several hundred cm^{-1} and spin-orbit splittings of similar magnitude. Thus, it is clear that these hot Raman transitions are amenable to experimental detection.

In summary, in this discussion we have analyzed the hot Raman transitions within the split manifolds of excited vibrational levels of Renner-Teller active modes in the absence as well as in the presence of spin-orbit coupling. We have shown that these hot Raman transitions are marked by polarizability tensors which are usually much larger than those characteristic for fundamental Raman transitions. This important feature would enable their experimental analysis despite their unfavorable Boltzmann factors which attenuates their spectral intensity. We have shown that the spectral patterns ensuing via intermediate states of different symmetry differ drastically. This effect may enable the assignment of excited electronic states by preresonance and resonance Raman scattering. Furthermore the analysis of hot Raman transitions would enable the study of Renner-Teller interactions as well as Jahn-Teller interactions[4] for those modes whose fundamental transitions are not allowed by Raman scattering. Moreover we should point out that some of these transitions are marked by inverse depolarization ratio resulting via antisymmetric transition tensors.[6,7,9-20]

Finally, we point out that the dependence of the intensity of the Raman scattering on the frequency of laser excitation for the depolarized hot Raman transitions is different from that corresponding to the transitions which exhibit inverse polarization. The expressions for these excitation profiles are given in Eqs. (III. 7), (III. 8), and (III. 12) for the Renner-Teller case without spin-orbit couplings, whereas, for the Renner-Teller case with spin-orbit couplings the excitation profiles are displayed in Eqs. (III. 17)-(III. 21)

[1] D. A. Long, *Raman Spectroscopy* (McGraw-Hill, New York, 1977), p. 4.
[2] R. Renner, Z. Phys. 92, 172 (1934); J. A. Pople and H. C. Longuet-Higgins, Mol. Phys. 1, 372 (1958); J. A. Pople, *ibid.* 3, 16 (1960).
[3] G. Herzberg, *Electronic Spectra and Electronic Structure of Polyatomic Molecules* (Van Nostrand, Princeton, 1966), pp. 23-37.
[4] B. Scharf and Y. B. Band, J. Chem. Phys. 79, 3175 (1983).
[5] J. Tang and A. C. Albrecht, in *Raman Spectroscopy*, edited by H. A. Szymanski (Plenum, New York, 1970), pp. 33-68.
[6] G. Placzek, *Marx Handbuch der Radiologie*, 2nd ed. (Akademische, Leipsig, 1934), Vol. 6(II), p. 209.
[7] Reference 1, pp. 120-124.
[8] Y. B. Band and B. M. Aizenbud, Chem. Phys. Lett. 77, 49 (1981); 79, 244 (1981).
[9] M. S. Child and H. C. Longuet-Higgins, Philos. Trans. R. Soc. London Ser. A 254, 259 (1961).
[10] O. S. Mortensen and J. A. Koningstein, J. Chem. Phys.

48, 3971 (1968).
[11]A. C. Albrecht, J. Chem. Phys. 34, 1476 (1961).
[12]J. A. Koningstein, Chem. Phys. Lett. 2, 31 (1968).
[13]W. M. McClain, J. Chem. Phys. 55, 2789 (1971).
[14]T. G. Spiro and T. C. Strekas, Proc. Natl. Acad. Sci. U.S.A. 69, 2622 (1972).
[15]D. W. Collins, D. B. Fitchen, and A. Lewis, J. Chem. Phys. 59, 5714 (1973).
[16]J. M. Friedman and R. M. Hochstrasser, Chem. Phys. 1, 457 (1973); Chem. Phys. Lett. 32, 414 (1975).
[17]A. L. Verma and H. J. Bernstein, J. Chem. Phys. 61, 2560 (1974).
[18]A. L. Verma, R. Mendelsohn, and H. J. Bernstein, J. Chem. Phys. 61, 383 (1974).
[19]O. S. Mortensen, Chem. Phys. Lett. 30, 406 (1975).
[20]L. D. Barron, Mol. Phys. 31, 129 (1976).